T2R2 東京科学大学 リサーチリポジトリ
Science Tokyo Research Repository

論文 / 著書情報
Article / Book Information

Title	A review of low density porous materials used in laser plasma experiments
Authors	Keiji Nagai, Christopher S. A. Musgrave, Wigen Nazarov
Citation	Physics of Plasmas, Vol. 25, No. 3, pp. 030501 1-14
Pub. date	2018, 3
Copyright	2018 Author(s). This article is distributed under a Creative Commons Attribution (CC BY) License.

Powered by T2R2 (Science Tokyo Research Repository)

A review of low density porous materials used in laser plasma experiments

Keiji Nagai, Christopher S. A. Musgrave, and Wigen Nazarov

Citation: Physics of Plasmas **25**, 030501 (2018); doi: 10.1063/1.5009689
View online: https://doi.org/10.1063/1.5009689
View Table of Contents: http://aip.scitation.org/toc/php/25/3
Published by the American Institute of Physics

Articles you may be interested in

Generation of controllable plasma wakefield noise in particle-in-cell simulations
Physics of Plasmas **24**, 103129 (2017); 10.1063/1.4986399

A comprehensive alpha-heating model for inertial confinement fusion
Physics of Plasmas **25**, 012703 (2018); 10.1063/1.4991405

Magnetic plasma expulsion
Physics of Plasmas **25**, 012508 (2018); 10.1063/1.5006887

Editorial: Preface to the 25th Volume of Physics of Plasmas
Physics of Plasmas **25**, 010401 (2018); 10.1063/1.5021964

The I-Raum: A new shaped hohlraum for improved inner beam propagation in indirectly-driven ICF implosions on the National Ignition Facility
Physics of Plasmas **25**, 012711 (2018); 10.1063/1.5010922

On the enhancement of p-^{11}B fusion reaction rate in laser-driven plasma by $\alpha \rightarrow$ p collisional energy transfer
Physics of Plasmas **25**, 020701 (2018); 10.1063/1.5007923

A review of low density porous materials used in laser plasma experiments

Keiji Nagai,[1] Christopher S. A. Musgrave,[1] and Wigen Nazarov[2]
[1]*Tokyo Institute of Technology, R1-26 Suzukake-dai, Midori-ku, Yokohama, Kanagawa 226-8503, Japan*
[2]*University of St. Andrews, North Haugh, St. Andrews, Fife, Scotland*

(Received 19 October 2017; accepted 20 February 2018; published online 16 March 2018)

This review describes and categorizes the synthesis and properties of low density porous materials, which are commonly referred to as foams and are utilized for laser plasma experiments. By focusing a high-power laser on a small target composed of these materials, high energy and density states can be produced. In the past decade or so, various new target fabrication techniques have been developed by many laboratories that use high energy lasers and consequently, many publications and reviews followed these developments. However, the emphasis so far has been on targets that did not utilize low density porous materials. This review therefore, attempts to redress this balance and endeavors to review low density materials used in laser plasma experiments in recent years. The emphasis of this review will be on aspects of low density materials that are of relevance to high energy laser plasma experiments. Aspects of low density materials such as densities, elemental compositions, macroscopic structures, nanostructures, and characterization of these materials will be covered. Also, there will be a brief mention of how these aspects affect the results in laser plasma experiments and the constrictions that these requirements put on the fabrication of low density materials relevant to this field. This review is written from the chemists' point of view to aid physicists and the new comers to this field. © *2018 Author(s). All article content, except where otherwise noted, is licensed under a Creative Commons Attribution (CC BY) license (http://creativecommons.org/licenses/by/4.0/).* https://doi.org/10.1063/1.5009689

I. INTRODUCTION

All low-density materials mentioned in this paper are porous with high surface areas. Strictly speaking, the definition of foam is air bubbles dispersed in a solid or liquid medium. Although it is used in this paper for ease of reading, foam is an oversimplified definition of low-density porous materials, which takes no account of the pore size, its distribution or whether it is an open or closed cell structure. It is a very general term and could apply to liquid foams as well. The International Union of Pure and Applied Chemistry (IUPAC) classifies porous materials into three categories.[1] (1) Microporous material, which is defined as having pore sizes less than 2 nm, (2) mesoporous materials, which have a pore size of 2–50 nm, and (3) macroporous materials with pore sizes above 50 nm. Almost all of the low density porous materials mentioned in this review fall within the category of macroporous materials.

In laser plasma experiments, low-density porous materials give a controlled low-density plasma, which produces an optically thin plasma, exhibiting the so-called volume heating effect and relatively uniform temperature and density compared with bulk materials.[2,3] Foams are useful not only for fundamental study, but also for applications to desirable temperature control. For example, such a low-density effect has been studied by using a double pulse scheme, where efficient x-ray generation was established 30 years ago using copper targets.[4] In this study, a comparison between cases with and without a pre-pulse shows a variation in ion energies by a factor of 2–4. More recently, practical extreme ultraviolet light sources for semiconductor lithography adopt a similar double pulse scheme to enhance the emission intensity with 100 kHz repetition.[5,6] However, it has a durability problem due to the difficulty of controlling a dynamic process caused by the pre-pulse expansion of liquid tin resulting in a low density target during the main pulse.[7] Generally, the gas phase has a density 3 orders lower than those of the liquid or solid, therefore a high pressure gas exhibits preferable density for laser absorption. By that reasoning, a gas puff target is promising in the production of low density plasma and it is possible to adopt into a high repetition laser[8–13] by using a high-pressure gas and a specially designed nozzle. This, however, is limited to few elements with the gaseous state.

Low density foam targets on the other hand, have a well defined geometry and density before laser illumination, and these have been used for laser-plasma interactions,[2,14,15] the study of laser shock measurements,[16–18] thermal smoothing effect,[19–22] quantum beam generation,[3,23] coulomb explosion,[24] and laboratory astrophysics.[25,26] Additionally, low density foams have been utilized as a mold of cryogenic targets.[27–31]

There have been several review papers on laser targets,[32–36] however, this paper is the first review focusing on low density materials used as laser targets. The authors believe that this review could be a good introduction to scientists that are starting to work in this field.

Foam fabrication techniques have also been investigated over a wide range of densities, element compositions, macroscopic structures, and nanostructures. These foam design, criteria and material selection are overviewed in Sec. II. Foams for laser targets are generally produced by various chemical synthetic methods *via* gel which is an interconnected network

 © Author(s) 2018.

TABLE I. Foam types used in laser targets and their properties.

Foam class	Pore size range[a]	Density range (mg/cm^3)[b]	Element composition	High/low Z (e1)	Target dimensions (μm)
Aerogels					
Organic aerogels (RF)	nm	10–250	CHO	Low Z	200–600
Inorganic aerogels	nm	1–250	(Si, Ta, Ga, Al) O_2	Middle-High Z	200–600
Carbonized aerogels	nm	10–250	C	Low Z	200–600
PolyHIPE	μm	30–250	CH	Low Z	200–600
Acrylates and Methacrylates	μm	5–250	CHO	Low Z	10–600
Templated foams	nm-μm	1–250	Metal oxides	High Z	10–600
Electrospinning	nm	1–250	Metal oxides	High Z	10–600
Poly(3-methyl-1-pentene)	nm-μm	3–250	CH_2	Low Z	200–600

[a]Except the template process, the pore size always has a distribution, and its dispersity depends on the synthesis condition.
[b]The density range shown here is not so strict and will enlarge by future development.

surrounded by a liquid. Because of the network structure, it loses translational motion of the polymer chains, and becomes a solid jelly-like material and exhibits no flow instead having a steady macroscopic shape. The final step in the synthesis involves the removal of liquid using a freeze drying technique,[37,38] or supercritical liquid CO_2 extraction.[39] The details of these processes depend on the materials due to the chemical interaction between the solvent and nanostructure of the skeleton and pore size of the gel. The material properties affect low density materials, such as shrinkage during synthesis and absorb humidity.[40] Then, the paper reviews each material property for target in the Sec. III. The target specification is not only materials, but also macroscopic shape and geometries. These fabrication processes are described in Sec. IV. Characterization is an important step in the preparation process of low-density materials and will be discussed at the end of this review.

II. DESIGN CRITERIA AND MATERIAL SELECTION FOR LOW-DENSITY TARGETS

Low density porous materials must possess a combination of properties in order to be useful for laser targets. Table I shows some of the low-density porous materials with their properties that have been utilized in laser experiments to date, and Fig. 1 is these mapping. Briefly these are density, pore diameter, element composition, and shape. Note that the description is not so exact and just an overview as

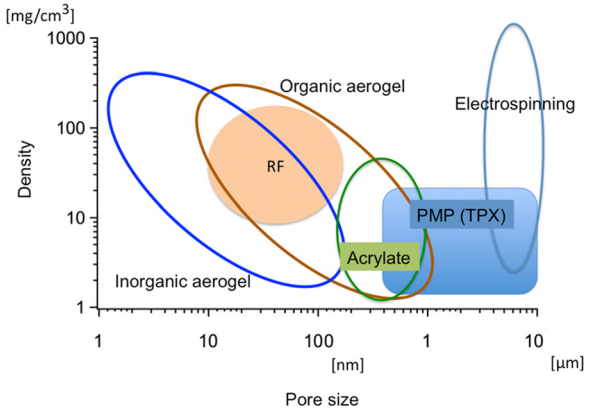

FIG. 1. Possible specification range of density versus pore size to synthesize as the laser target depending on materials.

mapping of materials. There is a wide range in these parameters, and depends on the material choice as experimental requirements. As for the mechanical strength, there are some aspects such as deformation and fracture. As a fabricated target, resistance to fracture is important because the target must keep the same shape until the laser irradiation. Shape is an important specification and the foams produced must either be capable of being synthesized inside the laser target or be strong enough for micro-machining into the desired shape.

There is a wide range of requirements on the elemental composition of low density materials for laser targets depending on the experimental requirements. Porous materials containing high atomic number (High Z) elements are required for some experiments, typically for high density compression and high temperature heating of plasma. Synthesis of targets containing high Z elements cannot be generalized due to uniquely different chemistry of these elements, which is based on an encyclopedic inorganic chemistry.[41] The most common inorganic low density middle and high Z targets utilized in laser experiments are SiO_2, Al_2O_3, TiO_2, SnO_2, and Ta_2O_5 aerogels, with many others reported in the literature.[42–45]

As for the materials choice, chemistry is an important parameter for designing target density and nanostructure size. If a target designer is not so interested in material chemistry, it would be a disadvantage in its target design. The highest density of foam is close to the solid density of the same material. Such high-density foam is similar to a polycrystalline material with nanometer to micrometer particle size, and differs from a single crystal in terms of optical transparency, macroscopic anisotropy, and mechanical properties. Currently, there is a great interest in high density porous materials in the form of a metal-organic framework with various functionalities,[46] and there are few examples that are of interest to laser targets.

On the other hand, the lower limit of the target density is around 1 mg/cm^3. One of the major constraints of producing such low-density materials for laser targets is the target size (<1 mm). This is due to high power laser focused spot size limitation, which are generally smaller than 1 mm, while almost all commercial porous materials have a large aspect ratio of void per frame materials.[47] The region of the lowest density of porous materials is comparable to the cut-off

density of plasma (n_{cr}), which allows the penetration and interaction of laser light with the frequency of ω_L, and the relation is as follows:[48]

$$\omega_L = \left[\left(e^2 n_{cr}\right)/\left(\varepsilon_0 m_e\right)\right]^{1/2}, \quad (1)$$

where e, ε_0, and m_e are the elementary charge, vacuum permittivity, and electron mass, respectively. This region is important because it allows penetration of the laser through the target and gives a so-called volume heating of the target, which gives an almost uniform density as the target density before expansion.[2,3]

In this review, the authors' definition of ultra-low density is materials with densities of lower than 10 mg/cm^{-3}. In order to obtain ultra-low densities, the removal of the solvent from a gel to the corresponding foam is achieved by the freeze-drying method or the supercritical fluid (SCF) extraction method; otherwise, the gel shrinks close to the corresponding solid density of the precursor. The freeze-dry method is a straightforward method to depend on the material used. When a low concentration gel was obtained, it will give densities in the region of 2.5 mg/cm^3,[37,38,49] however the resulting pore structure is ~20 μm size—too large for most laser target applications.

Generally, the lower the density of the foam the larger the pore size which sometimes could be larger than the laser spot size. This becomes a major difficulty for synthesizing low density narrow diameter pore size materials. Nano/micro structures of the target affect the properties of plasma.[50] The nanostructure control has been discussed in detail in terms of affinity of the polymer and solvent,[51,52] gelation kinetics,[51,53,54] containing nucleation and growth processes. The nucleation is based on equilibrium[55] or irreversibly formed seed such as adding particles, formation of chemical bonds, which can be introduced not only by simple mixing but also heating, light absorption, and pH change. The balance of the two processes governs the size and nanostructure of low-density materials. Generally, uniform and high density nuclear formation gives a finer structure size rather than the crystal growth parameter. In the review paper, three materials [polyacrylate, Poly(3-methyl-1-pentene) (PMP), and resorcinol formaldehyde (RF)] are discussed briefly to illustrate the point as examples.

III. LOW-DENSITY TARGET MATERIALS

A. Polyacrylate

A reliable material to give low density is acrylic foams,[56] which have been prepared from macro monomers containing multi vinyl groups and acrylates. To form the network structure, trimethylolpropane triacrylate (TMPTA, $C_{15}H_{20}O_6$) having three vinyl groups or ethylene glycol dimethacrylate (EGDM, $C_{10}H_{14}O_4$) having two vinyl groups are commonly used as a commercially available monomer source. As a reliable fabrication range, acrylic foams are generally used for the density range of 20–200 mg/cm^3 for various macroscopic shapes, while they can produce low density materials as low as 2 mg/cm^3 in a polymer container to keep the shape.[57] A viscous and soluble solvent with the monomers such as nonvolatile polyoxyethylene-4-lauryl ether (Brij 30) is chosen. The cross-linked acrylic polymer made by this technique exhibited a fine structure of ~200 nm.[58,59]

Borisenko *et al*. reported a polymer derived density gradient polyacrylate foam in a one-step interfacial polymerization process.[60,61] The components of that density gradient foam are 1,2-dichloromethane as the solvent, $SnCl_2$ as the initiator, and divinylbenzene as the monomer. There are two factors with this technique; (1) the solvent and monomer densities are different, 1.20 mg/cm^3 vs 0.91 mg/cm^3 respectively and (2) use of a capillary tube. The solvent and initiator are pre-mixed, and then the monomer is added. On addition of the solvent, the solvent and monomer separate based on the density, and polymerization begins on monomer contact with the solution due to the presence of the initiator. Once gelled, supercritical CO_2 drying removes the solvent to leave a polymer with a density gradient. The capillary tube acts as a pseudo-mold for the process (Fig. 2). Although they produced gradients as much as 400 mg/cm^3/mm, currently this method lacks the control to form prescribed density gradients.

B. Poly(3-methyl-1-pentene) (PMP)

PMP (poly(3-methyl-1-pentene) foams, also known by its commercial name TPX,[37,49,62–64] is of interest to laser physics experiments because it has a unique empirical formula CH_2 (polystyrene has a empirical formula CH). Low density materials with CH_2 empirical formula are valuable for opacity experiments. Additionally, PMP porous materials

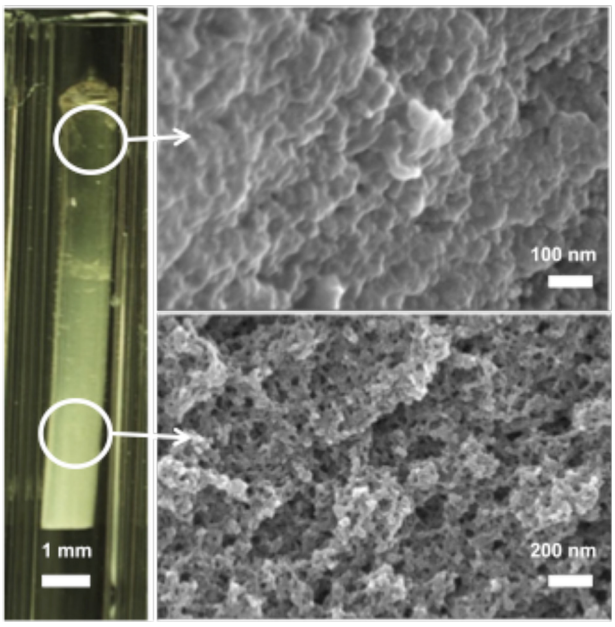

FIG. 2. (Left) A photo of a density gradient aerogel and the corresponding SEM images of the pore structure from two different areas of the gel. (Right) The SEM images demonstrate the morphology change from solid (top) to aerogel (bottom). The image above shows a cylindrical density gradient aerogel with a diameter of 1 mm and a length of 7 mm.[61] The gradient profile ranged from 1000 mg/cm^3 to 400 mg/cm^3. Reprinted with permission from Borisenko *et al*., J. Radioanal. Nucl. Chem. **299**, 961 (2014). Copyright 2014 Springer.

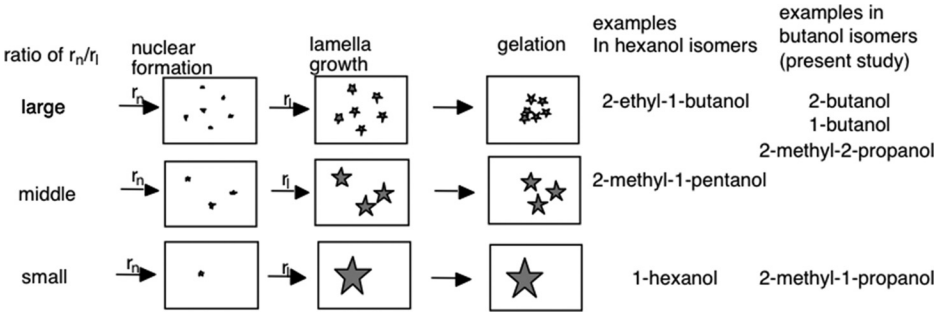

FIG. 3. Schematic view of the coagulation process in terms of nuclear formation and lamellar structure growth. The lamella size would be determined by the ratio of (r_n/r_l) and be correlated with affinity between the alkyl chain of alcohol and the side chain of poly(4-methyl-1-pentene). Reprinted with permission from Nagai *et al.*, Fusion Sci. Technol. **45**, 79–83 (2004). Copyright 2004 American Nuclear Society.[52]

also have the following properties: (1) no oxygen in their composition which interferes with X-ray diagnostics, (2) have the potential for heavy atom doping which are sometimes necessary for diagnostic reasons, and (3) they can be fabricated by dissolving the polymer in a hot solvent such as cyclohexane or decalin. Cyclohexane and decalin are good solvents for PMP at elevated temperatures due to their high boiling point. By cooling the solution, it solidified into ice. The ice can be dried *via* the freeze-drying technique (molecular distillation drying), which gave more than several micron pore size, to be porous PMP,[37,49] while those show larger pore sizes ($\sim$10 μm) than those dried by supercritical fluid extraction.

The pore size enlargement could be due to crystal growth of the solvent ice, or aggregation of the foam structure during the freeze drying process. The SCF drying minimizes the structure size to be in the 100 nm region. Furthermore, the size can be controlled by exchanging the cyclohexane solvent to non-volatile alcohol ($C_nH_{2n+1}OH$) derivatives ($n = 4$, 6),[51,52] where cyclohexane may be removed in the boiling condition of high boiling point alcohol. These alcohols have three roles: (1) immediate removal of the good solvent of cyclohexane, (2) density matching to PMP to avoid coagulation due to gravity, and (3) miscibility of the alcohol used in the process, with liquid CO_2 for SCF drying. By changing isomers of these alcohols, the affinity of the solvent to the side chain of the PMP branch structure can be controlled to avoid strong intermolecular interaction. The resultant crystal structure size can be explained with the interaction between the solvent branch and the side chain of PMP after SCF CO_2 extraction. Stronger interaction induced larger nanocrystalline size. Furthermore, a butanol derivative gave the finest crystal size at sub-micron, whilst keeping the density at 2–3 mg/cm^3.[52] Figure 3 is a schematic view of the mechanism.

C. Polysaccharides

Polysaccharide gel is commonly used for food and its processes. When the polysaccharide gel is dried, it becomes low density materials. A near critical density material is triacetate cellulose (TAC) and agar aerogel.[65] In the case of TAC, gelation depends on the freezing process and has an effect on the final nanostructure and mechanical strength. The lowest density of the material with a density of 1 mg/cm^3 was reported for a 150 μm thick film.[66]

Other systems such as cellulose derivatives have also been of interest. Polysaccharide derivatives have polar functional groups and have affinity to metal oxide precursors. An example of this is hydroxypropyl cellulose (HPC) solution, which forms a liquid crystal (LC) phase depending on the concentration in the solution. Because of its intrinsic LC phase and domain structure, metal oxides form a unique nanostructure after calcination. For example, 100-nm sized wavy crystal for HPC,[67] and an ellipsoidal crystal for ethyl-cyanoethyl cellulose.[68] It is worth noting that this cellulose derivative forms transparent films, and is a useful method for the mass production of a high repetition laser target (Fig. 4).[69]

D. Resorcinol formaldehyde (RF) and carbon aerogel

Resorcinol/formaldehyde (RF) aerogels have a phenolic structure made by a condensation reaction. They exhibit a fine structure (macroporous or mesoporous depending on the synthetic pathway) and have the advantage of being opaque to laser light. The RF aerogel was pioneered by Pekala,[70] and these low-density aerogels are synthesized in an aqueous system via the electrophilic aromatic substitution reaction by formaldehyde to resorcinol like the Friedel-Crafts condensation reaction.[71] Due to strong activation by two –OH groups, RF polymerization happens at room temperature *via* the base catalyzed reaction leads to a viscous solution, and pH change

FIG. 4. Rotating drum with coating HPC-Sn before (left) and after (right) 10 Hz laser irradiation. Reprinted with permission from Yasuda *et al.*, Fusion Sci. Technol. **49**, 691 (2006). Copyright 2006 American Nuclear Society.[67]

from neutral or acidic pH. This is a condensation reaction with resorcinol and formaldehyde, and in this reaction, resorcinol with a methylol group (-CH_2OH) is produced, and the methylol group reacts with another resorcinol. Such further addition of a methylol group to the aromatic ring extends the molecular weight and crosslinking. The typical range of density for these aerogels is 100–200 mg/cm^3, with thicknesses of 30–60 μm for the targets. RF aerogels with densities as low as 10 mg/cm^3 were reported.[42]

RF aerogels have an additional advantage of transparency to visible light (>600 nm), and are only composed of the elements carbon, hydrogen, and oxygen. RF's nanostructure can be controlled by the catalytic conditions, i.e., catalyst concentration, monomer concentration, and pH.[53] Larger pore sizes are obtained when the base catalyst to resorcinol ratio is increased ($215 < R/C < 450$), and it is also effective in decreasing the gelation time (>17 min) simultaneously. Acid catalyzed reactions also increase both the pore size and gelation time.[72] For example, a small amount of base catalyst, Na_2CO_3 (Resorcinol/Catalyst = 1500), formed a pore size of ~50 nm.[53,55]

Carbonized RF is of interest to a number of research fields including high energy density (HED) matter relating to battery and capacitor technology.[73–76] These carbonized materials are of interest because they contain only carbon and have the advantage of being the lowest Z composition porous materials possible. This can be achieved by furnace heating of RF aerogels.

E. Polystyrene and polyHIPE (High Internal Phase Emulsion)

Polystyrene has a simple element composition (C/H = 1) and great merits of a less expensive, amorphousness, transparency in the visible light region. A molecular design based on gelation control gives more flexibility to design low density targets. Divinyl benzene is basically a styrene monomer with an additional vinyl group on the aromatic ring, which gives the same polymer main chain as polystyrene and is used as a crosslinker for the synthesis of polystyrene foams.[77–79]

Due to high hydrophobicity, the polystyrene derivative can exhibit good phase separation with water, so-called High Internal Phase Emulsion (HIPE). PolyHIPE foams have relatively homogeneous pore distributions without a rigid template and high mechanical strengths.[80–82] Briefly, HIPEs are a combination of two immiscible liquids, generally known as the oil and water phases, which is stabilized by a surfactant. The hydrophobicity or lipophilicity of the surfactant determines what type of HIPE will be formed: oil-in-water (o/w) or water-in-oil (w/o). In most cases, emulsions relating to laser targets are of the o/w class of HIPE. In the production of porous materials using emulsions, the liquid that disperses inside the other liquid (called internal phase) is water and the liquid that contains the stabilized water is known as continuous phase. The continuous phase is a monomer or combination of monomers, which are polymerized after emulsification, and at the end of the process, the water (internal phase) is removed. The resultant structure has a well-defined open pore structure. The templated pores are typically 1–3 micrometers in diameter. The unique feature of HIPE synthesized foams is that these pores have "windows" originating from the volume contraction of the polymer. These "windows" have diameters of a couple hundreds of nanometers. PolyHIPEs also have the additional advantage of being stable and have high mechanical strengths meaning they are ideal for shaping them into simple laser targets using precision lathes.[81–85]

As described in the section of polyacrylate, generally volume shrinkage occurs during free-radical and photo-initiated polymerization. By contrast, cyclic carbonates and thiocarbonates undergo cationic and anionic ring opening polymerization resulting in volume expansion.[86–88] By combination of conventional free-radical polymerization and volume expansion ring opening polymerization, it would be possible to counteract the shrinkage with volume expansion during the polymerization process. A novel polystyrene-based low-density material with no shrinkage was synthesized and investigated.[88,89] The schematic concept is summarized in Fig. 5.

This process is carried out in two steps. The first step, styrene was copolymerized with styrene derivatives having a cyclic moiety to provide PS-based copolymers with a pendant cyclic moiety. In the second step, the linear PS-based copolymers are gelled by ring-opening polymerization of the

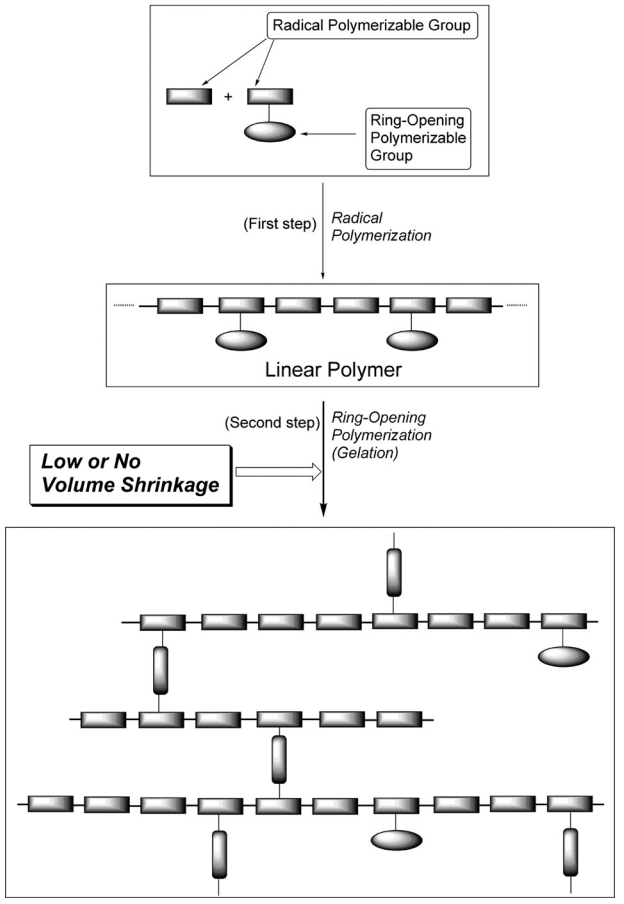

FIG. 5. Design of polystyrene based foam materials and process *via* radical copolymerization followed by cationic ring-opening polymerization. Reprinted with permission from Nemoto *et al.*, Fusion Sci. Technol. **49**, 695 (2006). Copyright 2006 American Nuclear Society.[89]

pendant cyclic moiety resulting in no volume change. For this purpose, two monomers 5-(4-vinylbenzyl) oxymethyl-5-methyl-1,3-dioxane-2-thione)[87] and 4-vinylphenyloxirane were synthesized,[88] and then used to synthesize polystyrene based copolymerization.

According to their systematic study to control the amount of crosslinker, the highest crosslinker gave the smallest shrinkage and the finest pore size down to 10 nm.[89,90] In the case of large cross linker groups, the nanostructure (50 nm) and shrinkage were small. Using smaller quantities of crosslinker (67%), increases the pore size to about 5 μm, with negligible shrinkage. On the other hand, the crosslinker (50%) gave rise to a large pore size and shrinkage. These results can be explained because of the high concentration of crosslinking molecules present rapidly forming many crosslinks, controlling the nanoporesize and without shrinkage.[90]

F. Ring opening metathesis polymerization (ROMP) aerogel

There have been in depth discussions regarding nanostructured aerogels and ring opening polymerization. The copolymerization of dicyclopentadienyl (DCPD) and norbornene (NB-R) with a different side group (R substituent group) caused a significant change in the morphology of the polymerized dicyclopentadienyl (PDCPD)-based aerogels. The incorporation of NB-R with a different substituent group could distort further growth of the primary polymerized dicyclopentadienyl (PDCPD) fibrils by either (i) decreasing the number of reactive sites (i.e., the crosslinking) at the surface or (ii) sterically hindering inter-particle crosslinking.[91]

The ROMP can be applied for thin polymeric porous low-density films through the sol-gel process. A monomer having multi-functional norbornene acts as the linker with a NR monomer, and the copolymer gave gel films where adding more NR monomers improved the uniformity of the gel films. The polymerization gives a viscous solution before its gelation. Aerogel coating with a uniform thickness from 10 μm to 100 μm was demonstrated.[91,92]

G. Metal oxide and metal halide

The precursors of metal oxide aerogels are their corresponding metal alkoxides, which are hydrolyzed and condensed into a metal oxide gel. Almost all of metal or semimetal oxides are known to form a gel. In a metal oxide aerogel, density and nanostructure control is not easy except for SiO_2, due to much faster hydrolysis rate of the alkoxide precursor except alkoxysilane.[42] In order to control the hydrolysis, propoxides and butoxides are used, and the water content also plays an important role. The hydrolysis rate of the precursor strongly depends on the element and there is less freedom to control them, nevertheless successful ZrO_2, Al_2O_3, Ta_2O_5, and SnO_2 have been reported.[42–45]

It is worth mentioning a beryllium hydride foam with sufficient strength for machining.[93] Beryllium hydride foams are very important in plasma physics experiments because of their high neutron yields.

H. Simple substance solid

A dry process without a solvent is a possible way to give relatively large microcrystals. Gromov *et al*. optimized the condition of vapor deposition, i.e., source temperature, chamber pressure and obtained a snowy metal like foam structure. Its macroscopic shape was controlled to the millimeter scale.[94,95]

A similar gas solvent process can be applied by spraying liquid Xe from a swirl atomizer into a low-pressure atmosphere to obtain low-density targets. Microparticles of liquid Xe were then rapidly cooled to a solid micrometer-sized powder. The predominant particle diameter was 100 μm under the liquid pressure of 0.3 MPa. The apparent density and production rate were 0.2 mg/cm^3 and 2.2 cm^3/s, respectively.[96]

I. Doping

For some laser plasma experiments, it is necessary to load or "dope" low Z porous materials with high Z elements, either as small diameter particles or using monomers with high Z elements. The level of these doping is usually 1–30 wt. % depending on the experimental requirements. Doping high Z elements into the structure of a hydrocarbon and subsequently into the polymer foam is sometimes a simple fabrication process, if the dopant required is in the particulate form. In an ultra-low density medium, the electron density of the high Z dopant can be higher than that of the host.[86] Such targets give a low-density effect of the high Z dopant, for example, high energy conversion efficiency from laser to x-ray. A ceramic based on SiO_2 and Spectraflux® mixed with varied amounts of another metal oxide such as (SnO_2) and heated in a tube furnace at temperatures between 900 and 1250 °C can produce a homogeneous dispersion of Sn in SiO_2.[97]

Organic foams with densities in the range 2–80 mg/cm^3 have been used as host materials for high Z doping. The choice of the host polymer depends on the elemental composition, nanostructure, density range, and other factors required for the experiment. The polarity of the side chain group is an important factor for uniform dispersion of nanoparticles.[98] The cross-linked acrylic polymer has a pore size of ~200 nm, and can be loaded with a variety of high Z elements containing co-monomers, such as chlorine and titanium.[99,100]

The RF foam possesses surface -OH groups which can induce hydrolysis to anchor metal oxide as another method for high Z doping. The doping in cases such as these is basically a surface template method.[101] PolyHIPEs, foams made from HIPE emulsions, are a suitable medium for some doping elements and dopants such as tungsten (W) and gold (Au) have been successfully loaded in polyHIPEs as shown in Fig. 6.[81]

IV. TARGET SHAPE, SIZE, AND GEOMETRY

A. General description

The shape, size, and geometry of the targets used in laser experiments are one of the crucial issues. It is a

boundary condition to characterize a laser-produced plasma such as its expansion and mixing before the laser absorption. There are two methods for achieving the required target dimensions and shape. One is mechanical machining using precision diamond tools and the second is *in-situ* molding, whereby the porous material is polymerized or "molded" inside the intended target vessel. Mechanical machining has developed significantly in the past decade or so and this method can produce complicated and intricate low-density targets.[43,102–105] A complicated structure, for example, a step-joined hemishell was fabricated by the mechanical machining technique, and discussed in detail elsewhere.[103] Laser machining is also a useful technique.[106,107] Machining, however, requires the material to have sufficient mechanical strength, resistance for deformation and fracture, to survive the process, for example polyHIPEs can be machined successfully.

Another useful method is a template process which does not depend on such optimization for each element. These processes have a capability to control the nanostructure and macroscopic structure, then they are described in Sec. IV G.

B. Molding porous materials into target shapes using chemical methods

The combination of molding and photopolymerization are powerful tools for the shaping of foam targets.[99] Using molds is also an effective method to form particularly complex shapes.[108–110]

The most common method used for molding is photoinitiated free radical polymerization of a multifunctional acrylic monomer (such as TMPTA) and photo-initiator (benzoin methyl ether), all dissolved in a solvent with low vapor pressure at room temperature. By exposing this solution of monomer and initiator to UV light, free radicals generate uniformly in the bulk. The polymerization by the uniform radical generation produces a uniform gel. The photoinitiation in this process induces fast and large crosslink density and results in low shrinkage with small pore size.[111] The main advantage of this method is that the precursor is a liquid

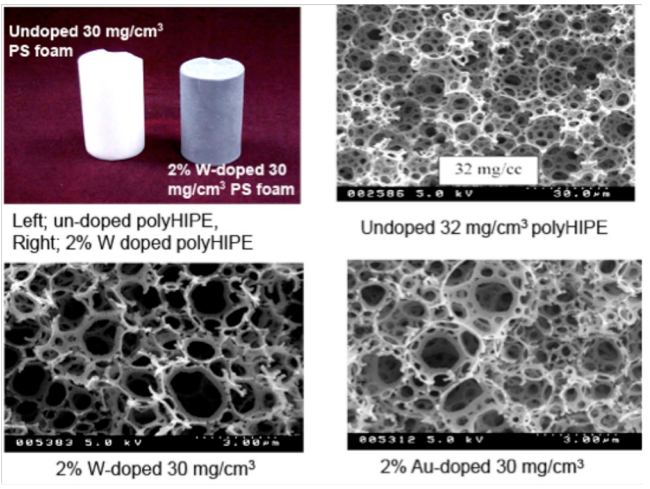

FIG. 6. SEM images of un-doped and doped W and Au polyHIPEs. Reprinted with permission from Steckle and Nobile, Fusion Sci. Technol. **43**, 301 (2003). Copyright 2007 American Nuclear Society.[81]

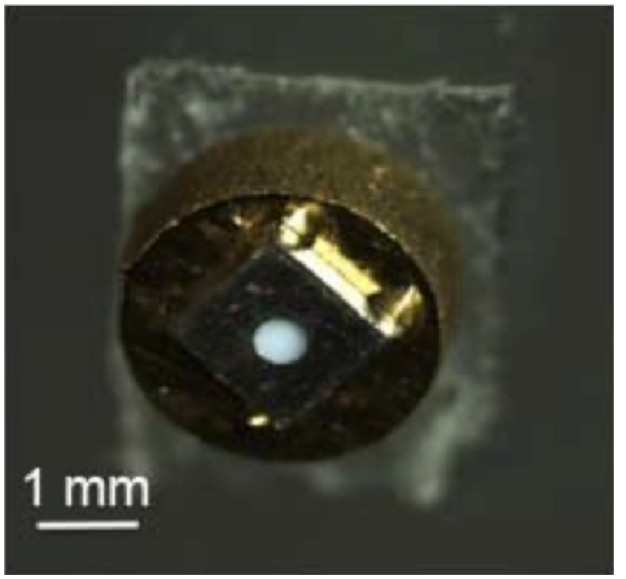

FIG. 7. A 3 mg/cm^3 acrylic foam, *in-situ* polymerized. Hole dimensions, 500 μm diameter, 200 μm depth. The washer was mounted on the gold block.

that can be injected into small cylinders, cavities, washers (see Figs. 6, 7 and 8), hohlraums, and other laser target components. Ultra low-density targets as low as 3 mg/cm^3 can be made using this technique.

In-situ polymerization is invaluable in filling of small target holes and cylinders with foam. A hollow cylinder or a small gap can be filled with a monomer solution containing a UV photoinitiator. When this solution is exposed to UV, the monomer solution polymerizes into a gel and the target is subsequently dried using a critical point dryer. This unique method produces targets that cannot be produced by any other physical or chemical technique. Monomers used for these targets are selected from a whole range of poly functional acrylic monomers.[112] There have been a number of targets filled with low density porous materials using this technique, sometimes as low as 5 mg/cm^3, with successful results investigating near-critical density controlled plasma produced from ultra-low-density plastic foam.[2] Figure 7 shows a small washer filled with 3 mg/cm^3 dried acrylic foam using the *in-situ* polymerization technique.

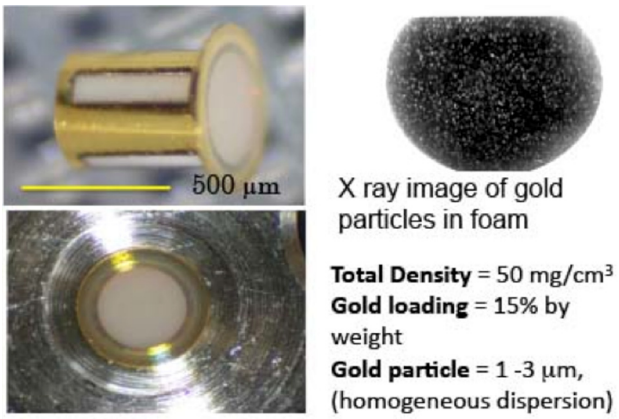

FIG. 8. Gold cylinder filled with low density foam, showing homogeneous gold particulate distribution.

Embedding objects in foam, a step-wise process[26,104] is deployed, while single step processes require a high viscosity precursor and rapid gelation is also possible.[110] The recent net-shape casting technique will open further investigation for the low density target, for example, an application for silica and ceramics has been investigated.[113]

Another advantage of this technique is the homogeneous dispersion of micron size metal particulates in the foam medium. It is possible to distribute gold particulates uniformly through the foam. A good example of this type target was developed for targets of the radiation transport experiment.[98] Figure 8 shows uniformly distributed gold particles in a low density foam, using the *in-situ* polymerization technique.

Crosslinking during polymerization is important, especially in low density porous materials to increase the strength of the porous structure. Crosslinking between polymer chains, however, results in conformation change, which leads to shrinkage. However, crosslinking high molecular weight polymer chains leads to less freedom of conformation and volume change. So, to avoid this shrinkage, a rapid and simultaneous formation of the crosslinked structure is useful, and it is realized by adding huge amounts of crosslinking photo-initiators or multi-functional monomers.[110]

C. Shell structure of low density materials

Hollow spherical geometry shells are the requirements for a number of laser experiments, particularly experiments involving plasma physics research relating to Inertial Confinement Fusion (ICF). An emulsion process is used for the production of these shells.[58] Viscosity control is crucial to controlling the thinness of the walls of these shells,[114] density matching method also plays an important part to achieve these high specifications.[115,116] In order to keep such a density matching and temperature independent reaction process, the phase transfer catalyst is a useful method.[117] Glass capsules with a silica coating were made by casting a glass capsule inside a solid block of SiO_2 aerogel with a density of 50 mg/cm^3, then the aerogel was diamond turned to a sphere of diameter 440 nm concentric to the embedded capsule.[118]

Hollow spherical shell structures with high specification are required for the isotropic implosion concept where isentropic compression is achieved by using a high power multi beam laser of the order of TW. A deuterium and tritium mixture used as the fuel in these experiments are very difficult to control because it has cryogenic boiling and melting temperatures of about 19 K. High quality shells with foam layers inside act as a container for the tritium/deuterium mixture.[27–31] The foam layer on the inner surface of the capsule acts as a wick to make the cryogenic fuel disperse as uniformly as possible. Since the foam thickness is constant, the thickness of the cryogenic fuel remains at a constant thickness. Therefore, homogeneity, density, and pore size of the foam become very important.[119] Emulsion processes can be optimized in order to adjust the sphericity and other important parameters for capsule production.[58,114–116,120–122]

A new approach was shown by Biener *et al*. as a coating inside the prefabricated spherical ablator capsule.[92] The aerogel precursor solution was P(DCPD-r-NB) as described in Sec. III F. The density was 25 mg/cm^3 without shrinking. The RF aerogel has the advantage of transparency, and RF capsules with large diameters were fabricated with a high degree of precision.[116,120,123–125] Because RF polymerization is carried out in aqueous solution, it emulsifies with the oil phase. Carbon in the final foam material was considered to be an acceptably low-content impurity for fusion plasma.[91]

D. Mass production of the low density film

Film targets are an indispensable method for future mass production of laser targets. With the recent developments in laser technology, there are an increasing number of high repetition rate (<100 Hz) systems. This of course will be incredibly challenging for more than 1 kHz solid state high repetition rate targets because producing large number of small dimensions of solid materials are *relatively* easier, since industrial processes have been producing such micro materials for decades. Therefore, for full density high repetition rate targets, it is only a question of miniaturization. However, mass synthesis of low density materials, with tight specifications of laser targets, has never been attempted before and possesses some unique challenges. At present, a large area film is a likely candidate to realize the high repetition laser illumination as shown in Fig. 4. Bearing in mind, that for the high repetition rate targets to be acceptable, all foam targets in the array must have little or no variation in terms of their density, dimensions, and structural morphology.

Electrospinning is a powerful mass production method for fabricating ultra-low density (<10 mg/cm^3) materials with a wide range of elemental compositions with mass production. The microstructure, density, and thickness of the metal-oxide fibers can be controlled by varying fabrication conditions.

As a typical example, a tin oxide nanofiber was prepared from a precursor of an ethanol solution of polyvinylpyrrolidone (PVP) and $SnCl_4$, as a support and metal source, respectively. Electrospinning can be performed in a simple (laboratory) set-up, however, a similar one is commercially available.[126] The precursor was loaded into a syringe equipped with a steel needle with an inner diameter of 0.5 mm. The needle was connected to a high-voltage supply capable of generating voltage up to 30 kV. The feeding rate of the precursor solution was controlled using an automatic syringe pump so that a small droplet was maintained at the needle tip.[127]

Usually, the nanofiber film is obtained as a large area (>cm^2) production. The thickness can be controlled because it is proportional to the feeding time, while the area control is not easy and cutting of the film is necessary for the preparation as a laser target.

Figure 9 shows examples of SnO_2 fibers, indicating a diameter range between 100 to 500 nm and a density range from 0.2 mg/cm^3 to 0.8 mg/cm^3.[127] The merit of the present method is mass production as a flat sheet structure. By

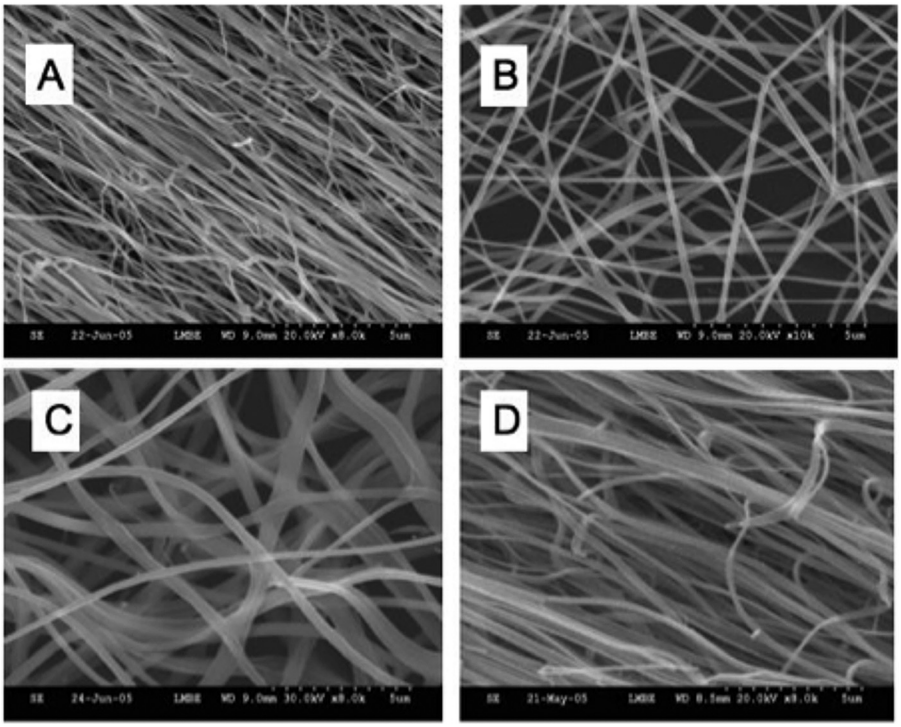

FIG. 9. SEM micrographs of SnO_2 mats. (a) $SnCl_4$ 2.5%, 180 ± 10 nm; (b) $SnCl_4$ 5%, 200 ± 10 nm; and (c) $SnCl_4$ 7.5%, 460 ± 10 nm. PVP concentration is 20% for the above three experiments. (d) PVP 40%, $SnCl_4$ concentration is 5%. All materials were calcined in air at 500 °C for 2 h. Reprinted with permission from J. Appl. Phys. **100**, 016104 (2006). Copyright 2006 AIP Publishing LLC.[127]

changing the metal source and other parameters, it is possible to synthesize various metal oxides such as vanadium and copper,[128] with densities as low as 20 mg/cm^3.

E. Control of the macroscopic shape

Accurate 3-D printers are currently used in density gradient materials. Jiang *et al.* and Oakdale *et al.* show direct writing via two photon polymerization (DLW-TPP) and printed millimeter-sized profiles with the density ranging from 0.06 to 0.6 g/cm^3.[129,130] They have the ability to design the size of the printed structures, polymer type, and pore size, meaning numerous synthetic possibilities, for example switching of layers of fragile low density materials.

F. Membrane on the porous material

Thin film coating is sometimes required as a gas barrier for cryogenic targets containing foams. Utilizing glues always has been a contentious issue in targets of this type, because commercial glues contain elements that could interfere with the results of the experiments.[110] Additionally, glue sometimes penetrates the pores in the porous structure and this leads to unpredictable density changes. Coating a film with foam is one effective way to overcome these problemx.[131] Also, there are some experiments where there is a request for coating a foam with a thin film. Low density foams by their very nature have pores, but laser experiments sometimes require porous materials to have a smooth surface. In order to overcome this dilemma, a thin layer whose size is less than the structure size is coated on the foam. A kind of surface polymerization on the liquid-liquid interface is necessary. In the interfacial polymerization reaction, crosslinking is one of the processes to obtain a uniform and thin membrane on the foam surface. Poly(4-vinylphenol) has been used as a coating layer by adding a phase transfer crosslinker of *m*-phthaloyldichloride.[58,59,131] The coating layer in this application was necessary to act as a gas barrier for foam-coated cryogenic targets. In order to produce such a barrier for RF aerogels, phase-transfer catalysis polymerization was used simultaneously during the gelation process. The polymerization of RF solution starts from the outer surface in contact with silicone oil containing a base phase-transfer catalyst.[117,132] Interestingly, acetic acid and propionic acid phase-transfer catalysts did not produce a membrane,[117] and hexanoic acid induced a membrane formation.[133]

G. Template processes to control micro and nanostructures

Template processes can control the nanostructure from 10 nm to several micrometers. This process can lead to mass productivity with less energy than the top down process. For example, the mono-dispersed and 100-nm-sized polymer particle template is a useful process for the preparation of porous materials. This is achieved by preparing a colloidal solution of the polymer particles and then casting onto a glass substrate and subsequently drying, resulting in a closed packed polymer template film. This process utilizes a liquid precursor that penetrates into the template. The composite film was then heated to decompose the polymer template to obtain a porous solid. A novel example is using metal oxides, such as $SnCl_4$ as a tin source. The $SnCl_4$ density was 1.5 g/cm^3, which was 23% of the density of the SnO_2 bulk (6.95 g/cm^3). The pore size was controlled by the template particle size.[134] In order to obtain a lower density, $SnCl_4$ was diluted with ethanol and water, as a precursor. After a similar process as described before, various morphologies were observed depending on the ratio of $SnCl_4$/ethanol whilst

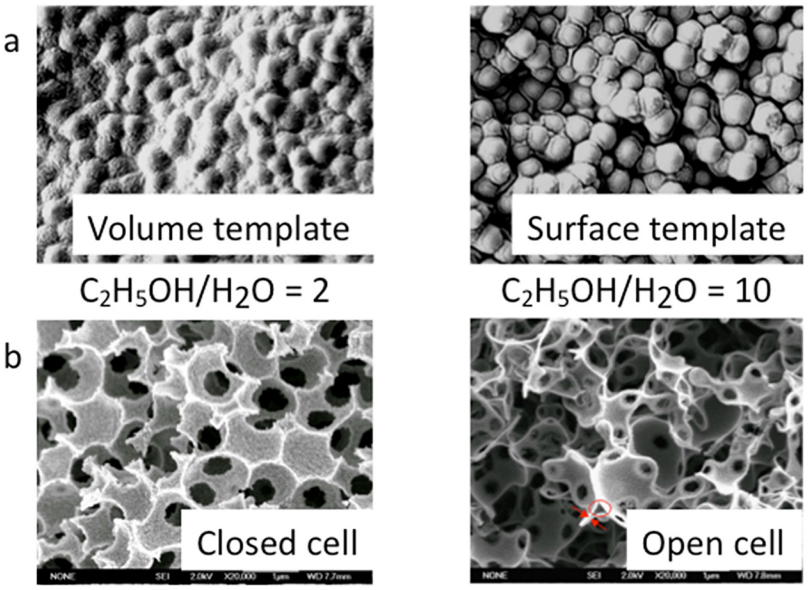

FIG. 10. (a) SEM images of volume template and surface templates on PS particles and (b) after removal of PS particles. Densities for both were 1.5 g/cm^3 SnO_2. Adapted with permission from Gu *et al.*, Chem. Mater. **17**, 1115 (2005). Copyright 2005 American Chemical Society.[134]

keeping the density at 0.5 g/cm^3 as shown in Fig. 10. The difference was classified into volume and surface template effects based on wettability differences of the precursor solution on the polymer particle.[134] These were utilized to study nanostructure differences of targets with keeping almost the same density.[135]

Nanoparticles smaller than the voids can be filled into the voids using a nanoparticles suspension.[109,136] A pure metallic tin foam was prepared using electrochemical plating on a PS particle membrane. The electrolyte for the tin plating consisted of $SnSO_4$ and *p*-phenol sulfonic acid in the presence of gelatin.[137] Voids can be filled with another material, for example lithium metal was filled by an electrochemical plating method.[138]

It is possible to control the macroscopic structure by combining the mono-disperse-sized nanoparticle template and microfluidic technique. Zhao *et al*. applied a microfluid device for a nanoparticle suspension, and obtained millimeter spheres of such nanoparticle aggregate with periodic packing.[139]

Highly ordered anodic porous alumina has a self-organized nanostructure prepared by an electrochemical process. It is a film template used to obtain a highly periodic and reliable structure template anode etched metal oxide (typically Al_2O_3) is used.[140,141] Lots of examples of exchanging materials are shown by Masuda *et al*.

For structures smaller than 100 nm, phase separation of block copolymers has been an established technique as a templating technique. It consists of a hydrophilic part and a hydrophobic part where each length is controlled by the catalyst and synthetic technique. The template provides a $<$100 nm sized structure as a periodic and thin membrane.[142–147]

The concept of the biotemplating process directly borrows from natural microstructures for new material fabrications. A use of three-dimensional helical feature in nature is an example of the biotemplate in which helical microalgae, *Spirulina* (*Arthrospira platensis*), a naturally shaping left-handed (LH) open helical structure, was utilized. Copper was coated via electroless plating onto the surface of *Spirulina* and the obtained coil had a micrometer pitch and diameter.[148] Another example is the direct use of *E-coli* cells. A few layers of micron sized bacteria coating on a polished surface increases the laser energy coupling and generates a hotter plasma which is effective for the ion acceleration.[149]

V. CHARACTERIZATION

In order to have a reliable and meaningful result that can be interpreted, experimentalists must know all parameters of the target materials used in the experiment. Target characterization is therefore an important step for the analysis of laser plasma in terms of density, element composition, geometry including pore size, porosity, and homogeneity. Density is estimated by the use of x-ray absorption, while visible light-scattering is used for large pore size. Such transmittance gives information on shape by the use of the imaging technique.[150] It is possible to establish the density by X-ray imaging,[56,57,84,98,111,151,152] a monochromatic X-ray source gives high resolution. For calibration, known samples are used. Direct measurement of density is based on measuring the mass and volume using an accurate microbalance, but this requires a sufficient quantity of the material with a well-defined geometry. As for the elemental composition, chemical analysis is not suitable as it requires a large quantity ($>$10 mg) to measure for one piece of target, but it is possible for the source material or if a huge quantity of targets are available.[125] Surface roughness can be monitored by scanning electron microscopy (SEM) and atomic force microscopy (AFM).[153,154] Energy dispersion x-ray (EDX) gives element composition qualitatively, however this gives information only for the focusing area, not the whole target. The visible light optical interferometric technique can be used to characterize not only the surface image, but also the thickness and density uniformity. It is, however, limited by scattering caused by the foam structure. Grazing incident small angle x-ray scattering (GISAXS) is a typical method for nanostructure characterization for the full target size,

especially taken at the interval, period sample having Bragg diffraction for the periodic sample, while the average nanostructure is obtained from it.[155] The use of solid state nuclear magnetic resonance (NMR) relaxometry is a promising new technique, which gives information about the structure of the polymer based on different orders of molecular motion.[83] Nitrogen adsorption and desorption according to Brunauer, Emmett and Teller (BET) specific surface area, distributions of pore radii. Other porosimetry also gives such information on pore distribution such mercury porosimetry, or even image analysis using the software. These characterizations are similar to higher order structure analysis in polymer physics,[156] which discusses the relation between the first order structure, chemical bond, and interaction between polymeric chains, macroscopic size, and nanostructure.

VI. SUMMARY

This review paper is focused on low density porous materials used for laser experiments and their properties relating to synthetic techniques, from the point of view of a material chemist synthesizing these materials. The relation between material chemistry and plasma physics is a key issue and this paper attempted to show both views. The paper would be expected to help the communication between the material chemist and experimental plasma physicist, designing targets for high energy lasers throughout the world. Most publications to date concentrated on non-porous materials, and this paper attempts to highlight some of the difficulties that are by in large very different than other types of targets. Hopefully, this review paper will help the experimentalists and the beginners to this field equally.

Materials synthesized for laser targets and HED physics experiments are very challenging, and in many cases, extremely unique and often with conflicting and demanding specifications. Quite often, the materials requested by the experimentalist are not commercially available and therefore need to be synthesized specifically for that/those experiment(s). Even if some materials are available, they cannot be used as supplied, and in most cases, they have to be adapted and miniaturized in order to fit the experimental requirements. Generally, because there are vastly diverse fields in HED physics and different specifications for different experiments, it is not always easy to gauge the future requirements. For these reasons, it is hoped that this review will demonstrate the challenges of making porous materials in this field and hopefully both groups, the users and the community that supplies these materials, will find this review beneficial. Dedicated target research is one option, exploring new materials science that spans not only HED physics, but other fields that require low density porous materials. This level of research could be self-sufficient, rather than relying on budget restricted experimental campaigns.

ACKNOWLEDGMENTS

We thank the Grant-in-Aid for Scientific Research (KAKENHI) and the Dynamic Alliance for Open Innovation Bridging Human, Environment and Materials from MEXT.

[1]K. S. W. Sing, D. H. Everett, R. A. W. Haul, L. Moscou, R. A. Pierotti, J. Rouquérol, and T. Siemieniewska, Pure Appl. Chem. **57**, 603 (1985).
[2]S. N. Chen, T. Iwawaki, K. Morita, P. Antici, S. D. Baton, F. Filippi, H. Habara, M. Nakatsutsumi, P. Nicolaï, W. Nazarov, C. Rousseaux, M. Starodubstev, K. A. Tanaka, and J. Fuchs, Sci. Rep. **6**, 21495 (2016).
[3]M. Tanabe, H. Nishimura, S. Fujioka, K. Nagai, N. Yamamoto, Z.-Z. Gu, C. Pan, F. Girard, M. Primout, B. Villette, D. Brebion, K. B. Fournier, A. Fujishima, and K. Mima, Appl. Phys. Lett. **93**, 051505 (2008).
[4]R. Kodama, T. Mochizuki, K. A. Tanaka, C. Yamanaka, and W. Sasaki, Appl. Phys. Lett. **50**, 720 (1987).
[5]J. Fujimoto, T. Abe, S. Tanaka, T. Ohta, T. Hori, T. Yanagida, H. Nakarai, and H. Mizoguchi, J. Micro/Nanolithogr., MEMS, MOEMS **11**, 021111 (2012).
[6]B. Rollinger, N. Gambino, D. Hudgins, A. Sanders, M. Brandstätter, R. S. Abhari, and F. Abreau, Proc. SPIE **9422**, 94222K (2015).
[7]A. Sunahara, Oyo Buturi **83**, 741–746 (2014) (in Japanese), see https://www.jsap.or.jp/ap/2014/09/ob830741-e.xml.
[8]Y. Fukuda, A. Ya. Faenov, M. Tampo, T. A. Pikuz, T. Nakamura, M. Kando, Y. Hayashi, A. Yogo, H. Sakaki, T. Kameshima, A. S. Pirozhkov, K. Ogura, M. Mori, T. Zh. Esirkepov, J. Koga, A. S. Boldarev, V. A. Gasilov, A. I. Magunov, T. Yamauchi, R. Kodama, P. R. Bolton, Y. Kato, T. Tajima, H. Daido, and S. V. Bulanov, Phys. Rev. Lett. **103**, 165002 (2009).
[9]H. Fiedorowicz, A. Bartnik, H. Daido, I.-W. Choi, M. Suzuki, and S. Yamagami, Opt. Commun. **184**, 161 (2000).
[10]A. McPherson, B. D. Thompson, A. B. Borisov, K. Boyer, and C. K. Rhodes, Nature **370**, 631 (1994).
[11]T. Ditmire, T. Donnelly, R. W. Falcone, and M. D. Perry, Phys. Rev. Lett. **75**, 3122 (1995).
[12]J. Zweiback, R. A. Smith, T. E. Cowan, G. Hays, K. B. Wharton, V. P. Yanovsky, and T. Ditmire, Phys. Rev. Lett. **84**, 2634 (2000).
[13]E. Miura, H. Honda, K. Katsura, E. Takahashi, and K. Kondo, Appl. Phys. B **70**, 783 (2000).
[14]T. Iwawaki, H. Habara, S. Baton, K. Morita, J. Fuchs, S. Chen, M. Nakatsutsumi, C. Rousseaux, F. Filippi, W. Nazarov, and K. A. Tanaka, Phys. Plasmas **21**, 113103 (2014).
[15]N. G. Borisenko and Y. A. Merkuliev, J. Russ. Laser Res. **31**, 256 (2010).
[16]K. Takamatsu, N. Ozaki, K. A. Tanaka, T. Ono, K. Nagai, M. Nakai, T. Watari, A. Sunahara, M. Nakano, T. Kataoka, H. Takenaka, M. Yoshida, K. Kondo, and T. Yamanaka, Phys. Rev. E **67**, 056406 (2003).
[17]D. Batani, A. Balducci, W. Nazarov, T. Löwer, T. Hall, M. Koenig, B. Faral, A. Benuzzi, and M. Temporal, Phys. Rev. E **63**, 046410 (2001).
[18]D. Batani, R. Dezulian, R. Redaelli, R. Benocci, H. Stabile, F. Canova, T. Desai, G. Lucchini, E. Krousky, K. Masek, M. Pfeifer, J. Skala, R. Dudzak, B. Rus, J. Ullschmied, V. Malka, J. Faure, M. Koenig, J. Limpouch, W. Nazarov, D. Pepler, K. Nagai, T. Norimatsu, and H. Nishimura, Laser Part. Beams **25**, 127 (2007).
[19]M. Kalal, J. Limpouch, E. Krousky, K. Masek, K. Rohlena, P. Straka, J. Ullschmied, A. Kasperczuk, T. Pisarczyk, S. Y. Gas'kov, A. I. Gromov, V. B. Rozamov, and V. N. Kondrashov, Fusion Sci. Technol. **43**, 275 (2003).
[20]N. Rudraiah, Fusion Sci. Technol. **43**, 307 (2003).
[21]T. Watari, M. Nakai, H. Azechi, T. Sakaiya, H. Shiraga, K. Shigemori, S. Fujioka, K. Otani, K. Nagai, A. Sunahara, H. Nagatomo, and K. Mima, Phys. Plasmas **15**, 092109 (2008).
[22]S. Depierreux, C. Labaune, D. T. Michel, C. Stenz, P. Nicolaï, M. Grech, G. Riazuelo, S. Weber, C. Riconda, V. T. Tikhonchuk, P. Loiseau, N. G. Borisenko, W. Nazarov, S. Hüller, D. Pesme, M. Casanova, J. Limpouch, C. Meyer, P. Di-Nicola, R. Wrobel, E. Alozy, P. Romary, G. Thiell, G. Soullié, C. Reverdin, and B. Villette, Phys. Rev. Lett. **102**, 195005 (2009).
[23]F. Pérez, A. Debayle, J. Honrubia, M. Koenig, D. Batani, S. D. Baton, F. N. Beg, C. Benedetti, E. Brambrink, S. Chawla, F. Dorchies, C. Fourment, M. Galimberti, L. A. Gizzi, L. Gremillet, R. Heathcote, D. P. Higginson, S. Hulin, R. Jafer, P. Koester, L. Labate, K. L. Lancaster, A. J. MacKinnon, A. G. MacPhee, W. Nazarov, P. Nicolai, J. Pasley, R. Ramis, M. Richetta, J. J. Santos, A. Sgattoni, C. Spindloe, B. Vauzour, T. Vinci, and L. Volpe, Phys. Rev. Lett. **107**, 065004 (2011).
[24]S. Okihara, T. Zh. Esirkepov, K. Nagai, S. Shimizu, F. Sato, T. Iida, K. Nishihara, T. Norimatsu, Y. Izawa, and S. Sakabe, Phys. Rev. E **69**, 026401 (2004).
[25]B. Loupias, M. Koenig, E. Falize, S. Bouquet, N. Ozaki, A. Benuzzi-Mounaix, T. Vinci, C. Michaut, M. Rabec le Goahec, W. Nazarov, C.

Courtois, Y. Aglitskiy, A. Ya. Faenov, and T. Pikuz, Phys. Rev. Lett. **99**, 265001 (2007).
[26]Y.-G. Kang, K. Nishihara, H. Nishimura, H. Takabe, A. Sunahara, T. Norimatsu, K. Nagai, H. Kim, M. Nakatsuka, H. J. Kong, and N. J. Zabusky, Phys. Rev. E **64**, 047402 (2001).
[27]T. Norimatsu, H. Katayama, T. Mano, M. Takagi, R. Kodama, K. A. Tanaka, Y. Kato, T. Yamanaka, S. Nakai, Y. Nishino, M. Nakai, and C. Yamanaka, J. Vac. Sci. Technol. A **6**, 3144 (1988).
[28]R. A. Sacks and D. H. Darling, Nucl. Fusion **27**, 447 (1987).
[29]A. Iwamoto, T. Fujimura, M. Nakai, T. Norimatsu, H. Sakagami, H. Shiraga, and H. Azechi, Nucl. Fusion **53**, 083009 (2013).
[30]A. Richard, K. A. Tanaka, K. Nishihara, M. Nakai, M. Katayama, Y. O. Fukuda, T. Kanabe, Y. Kitagawa, T. Norimatsu, M. Nakatsuka, T. Yamanaka, M. Kado, T. Kawashima, C. Chen, M. Tsukamoto, and S. Nakai, Phys. Rev. E **49**, 1520 (1994).
[31]R. E. Olson, R. J. Leeper, J. L. Kline, A. B. Zylstra, S. A. Yi, J. Biener, T. Braun, B. J. Kozioziemski, J. D. Sater, P. A. Bradley, R. R. Peterson, B. M. Haines, L. Yin, L. F. Berzak Hopkins, N. B. Meezan, C. Walters, M. M. Biener, C. Kong, J. W. Crippen, G. A. Kyrala, R. C. Shah, H. W. Herrmann, D. C. Wilson, A. V. Hamza, A. Nikroo, and S. H. Batha, Phys. Rev. Lett. **117**, 245001 (2016).
[32]T. Norimatsu, D. Harding, R. Stephens, A. Nikroo, R. Petzoldt, H. Yoshida, K. Nagai, and Y. Izawa, Fusion Sci. Technol. **49**, 483 (2006).
[33]T. Norimatsu, K. Nagai, T. Yamanaka, T. Endo, H. Yoshida, and Y. Sakagami, Fusion Eng. Des. **63**, 587 (2002).
[34]K. Nagai, T. Norimatsu, Y. Izawa, and T. Yamanaka, "Laser fusion target nanomaterials," in *Encyclopedia of Nanoscience and Nanotechnology*, edited by E. H. Nalwa (American Scientific Publishers, Stevenson Ranch, CA, 2004), Vol. 4, pp. 407–419, ISBN: 1-58883-060-8
[35]I. Prencipe, J. Fuchs, S. Pascarelli, D. Shumacher, R. B. Stephens, N. B. Alexander, R. Briggs, M. Büscher, M. O. Cernaianu, A. Choukourov, M. De Marco, A. Erbe, J. Fassbender, G. Fiquet, P. Fitzsimmons, C. Gheorghiu, J. Hund, L. G. Huang, M. Harmand, N. Hartley, A. Irman, T. Kluge, Z. Konopkova, S. Kraft, D. Kraus, V. Leca, D. Margarone, J. Metzkes, K. Nagai, W. Nazarow, P. Lutoslawski, D. Papp, M. Passoni, A. Pelka, J. P. Perin, J. Schulz, M. Smid, C. Spindloe, S. Steinke, R. Torchio, C. Vass, T. Wiste, R. Zaffino, K. Zeil, T. Tschentscher, U. Schramm, and T. E. Cowan, High Power Laser Sci. Eng. **5**, e17 (2017).
[36]Y. Izawa and T. Norimatsu, in *Nuclear Fusion by Inertial Confinement*, edited by G. Velarde, Y. Ronen, and J. M. Martinez-Val (CRC Press, Boca Raton, 1993), p. 515.
[37]W. L. Perry, R. C. Dye, P. G. Apen, L. Foreman, and E. Peterson, Appl. Phys. Lett. **66**, 314 (1995).
[38]K. Okada, S. Sakabe, H. Shiraga, T. Mochizuki, and C. Yamanaka, Jpn. J. Appl. Phys., Part 2 **21**, L257 (1982).
[39]M. McHugh and V. Krukonis, *Supercritical Fluid Extraction*, 2nd ed. (Elsevier, 2013).
[40]C. E. Hamikton, N. A. Smith, J. R. Schoonover, K. A. D. Obrey, N. Bazin, and T. Jewell, Fusion Sci. Technol. **63**, 301 (2011).
[41]P. W. Atkins, T. L. Overton, J. P. Rourke, M. T. Weller, and F. A. Armstrong, *Shriver and Atkins' Inorganic Chemistry*, 5th ed. (Oxford University Press, 2010).
[42]N. Hüsing and U. Schubert, Angew. Chem., Int. Ed. **37**, 22 (1998).
[43]J. F. Hund, R. R. Paguio, C. A. Frederick, A. Nikroo, and M. Thi, Fusion Sci. Technol. **49**, 669 (2006).
[44]J. F. Hund, J. McElfresh, C. A. Frederick, A. Nikroo, A. L. Greenwood, and W. Luo, Fusion Sci. Technol. **51**, 701 (2007).
[45]C. A. Frederick, A. C. Forsman, J. F. Hund, and S. A. Eddinger, Fusion Sci. Technol. **55**, 499 (2009).
[46]H.-C. Zhou and S. Kitagawa, Chem. Soc. Rev. **43**, 5415 (2014).
[47]K. W. Suh, C. P. Park, M. J. Maurer, M. H. Tusim, R. D. Genova, R. Broos, and D. P. Sophiea, Adv. Mater. **12**, 1779 (2000).
[48]F. F. Chen, *Introduction to Plasma Physics and Controlled Fusion*, 3rd ed. (Springer, 2016).
[49]A. J. Antolak, D. H. Morse, D. E. Hebron, R. J. Leeper, and D. Schroen-Carey, Fusion Eng. Des. **46**, 37 (1999).
[50]H. Habara, S. Honda, M. Katayama, H. Sakagami, K. Nagai, and K. A. Tanaka, Phys. Plasmas **23**, 063105 (2016).
[51]K. Nagai, B.-R. Cho, Y. Hashishin, T. Norimatsu, and T. Yamanaka, Jpn. J. Appl. Phys., Part 2 **41**, L431 (2002).
[52]K. Nagai, T. Norimatsu, and Y. Izawa, Fusion Sci. Technol. **45**, 79–83 (2004).
[53]C. A. Frederick, R. R. Paguio, A. Nikroo, J. H. Hund, O. Accennas, and M. Thi, Fusion Sci. Technol. **49**, 657 (2006).
[54]D. Kashchiev, *Nucleation, Basic Theory with Applications* (Butterworth-Heinemann, 2000).
[55]R. Petricevic, G. Reichenauer, V. Beck, A. Emmerling, and J. Fricke, J. Non-Cryst. Solids **225**, 41 (1998).
[56]J. W. Falconer, W. Golnazarians, M. J. Baker, and D. W. Sutton, J. Vac. Sci. Technol. A **8**, 968 (1990).
[57]J. W. Falconer, W. Nazarov, and C. J. Horsfield, J. Vac. Sci. Technol. A **13**, 1941 (1995).
[58]M. Takagi, M. Ishihara, T. Norimatsu, Y. Izawa, and S. Nakai, J. Vac. Sci. Technol. A **11**, 2837 (1993).
[59]C. Chen, T. Norimatsu, M. Takagi, H. Katayama, T. Yamanaka, and S. Nakai, J. Vac. Sci. Technol. A **9**, 340 (1991).
[60]N. G. Borisenko, W. Nazarov, C. Musgrave, Y. A. Merkuliev, A. Orekhov, and L. A. Borisenko, J. Radioanal. Nucl. Chem. **299**, 961 (2014).
[61]L. Borisenko, A. Orekhov, C. Musgrave, W. Nazarov, Y. A. Merkuliev, and N. Borisenko, J. Phys.: Conf. Ser. **713**, 012009 (2016).
[62]M. Grosse, L. Guillot, B. Reneaume, E. Fleury, C. Hurmerel, A. Choux, L. Jeannot, I. Geoffray, A. Faivre, O. Breton, J. Andre, R. Collier, and O. Legaie, Fusion Sci. Technol. **59**, 205 (2011).
[63]M. A. Mitchell, P. Gobby, and N. Elliott, Fusion Technol. **28**, 1844 (1995).
[64]I. G. Schneir and B. McQuillan, Fusion Technol. **28**, 1849 (1995).
[65]N. G. Borisenko, I. V. Akimova, A. I. Gromov, A. M. Khalenkov, Y. A. Merkuliev, V. N. Kondrashov, J. Limpouch, E. Krousky, W. Nazarov, and V. F. Petrunin, Fusion Sci. Technol. **49**, 676 (2006).
[66]V. G. Pimenov, E. E. Sheveleva, and A. M. Sakharov, Instrum. Exp. Tech **59**, 321 (2016).
[67]Y. Yasuda, Q. Gu, K. Nagai, M. Nakai, T. Norimatsu, S. Fujioka, H. Nishimura, and M. Nakatsuka, Fusion Sci. Technol. **49**, 691 (2006).
[68]Q. Gu, K. Nagai, M. Nakai, and T. Norimatsu, Colloid Polym. Sci. **284**, 429 (2006).
[69]K. Nagai, Q. Gu, Y. Yasuda, T. Norimatsu, S. Fujioka, H. Nishimura, N. Miyanaga, Y. Izawa, and K. Mima, J. Polym. Sci.: Part A: Polym. Chem. **47**, 4566 (2009).
[70]R. W. Pekala, J. Mater. Sci. **24**, 3221 (1989).
[71]Session 16.3. Alkylation and Acylation of Aromatic Rings: The Friedel-Crafts Reaction, p. 554; J. McMurry, *Organic Chemistry*, 7th ed. (Thomson Learning, 2008).
[72]R. Saliger, U. Fischer, C. Herta, and J. Fricke, J. Non-Cryst. Solids **225**, 81 (1998).
[73]L. Chuenchom, R. Kraehnert, and B. M. Smarsly, Soft Matter **8**, 10801 (2012).
[74]Y. Tao, M. Endo, M. Inagaki, and K. Kaneko, J. Mater. Chem. **21**, 313 (2011).
[75]W. Gu and G. Yushin, WIREs Energy Environ. **3**, 424 (2014).
[76]S. A. Al-Muhtaseb and J. A. Ritter, Adv. Mater. **15**, 101 (2003).
[77]J. Streit and D. Schroen, Fusion Sci. Technol. **43**, 321 (2003).
[78]C. E. Hamilton, M. N. Lee, and A. N. G. Parra-Vasquez, Fusion Sci. Technol. **70**, 226 (2016).
[79]R. R. Paguio, A. Nikroo, M. Takagi, and O. Acenas, J. Appl. Polym. Sci. **101**, 2523 (2006).
[80]N. Elliott, C. W. Barnes, S. H. Batha, R. D. Day, J. Elliott, P. Gobby, V. Gomez, D. Hatch, N. E. Lanier, G. R. Magelssen, R. Manzanares, R. Perea, T. Pierce, G. Rivera, D. Sandoval, J. M. Scott, W. Steckle, D. L. Tubbs, S. Rothman, C. Horefield, A. M. Dunne, and K. W. Parker, Fusion Sci. Technol. **41**, 196 (2002).
[81]W. P. Steckle and A. Nobile, Fusion Sci. Technol. **43**, 301 (2003).
[82]W. P. Steckle, M. E. Smith, R. J. Sebring, and A. Nobile, Fusion Sci. Technol. **45**, 74 (2004).
[83]N. G. Borisenko, A. A. Akunets, I. A. Artyukov, K. E. Gorodnichev, and Y. A. Merkuliev, Fusion Sci. Technol. **55**, 477 (2009).
[84]C. S. A. Musgrave, W. Nazarov, and N. Bazin, J. Mater. Sci. **52**, 3179 (2017).
[85]K. L. Anderson, W. Nazarov, C. S. A. Musgrave, N. Bazin, and D. Faith, J. Radioanal. Nucl. Chem. **299**, 969 (2014).
[86]T. Takata and T. Endo, Prog. Polym. Sci. **18**, 839 (1993).
[87]N. Nemoto, F. Sanda, and T. Endo, Macromolecules **33**, 7229 (2000).
[88]N. Nemoto, F. Sanda, and T. Endo, J. Polym. Sci.: Part A: Polym. Chem. **39**, 1305 (2001).
[89]N. Nemoto, K. Nagai, Y. Ono, K. Tanji, T. Tanji, M. Nakai, and T. Norimatsu, Fusion Sci. Technol. **49**, 695 (2006).

[90]K. Yamanaka, K. Nagai, N. Nemoto, K. Nomura, T. Shimomura, K. Tanji, M. Nakai, and T. Norimatsu, Fusion Sci. Technol. **51**, 665 (2007).
[91]S. H. Kim, M. A. Worsley, C. A. Valdez, S. J. Shin, C. Dawediet, T. Braum, T. F. Baumann, S. A. Letts, S. O. Kucheyev, K. J. J. Wu, J. Biener, J. H. Satcher, and A. V. Hamza, RSC Adv. **2**, 8672 (2012).
[92]J. Biener, C. Dawedeit, S. H. Kim, T. Braun, M. A. Worsley, A. A. Chernov, C. C. Walton, T. M. Willey, S. O. Kucheyev, S. J. Shin, Y. M. Wang, M. M. Biener, J. R. I. Lee, B. J. Kozioziemski, T. van Buuren, K. J. J. Wu, J. H. Satcher, Jr., and A. V. Hamza, Nucl. Fusion **52**, 062001 (2012).
[93]N. G. Borisenko, V. M. Dorogotovtsev, A. I. Gromov, S. Y. Guskov, Y. A. Merkul'ev, N. A. Chirin, A. Shikov, and V. F. Perrunin, Fusion Technol. **38**, 161 (2000).
[94]N. G. Borisenko, A. M. Khalenkov, V. Kmetik, Y. A. Merkuliev, and V. G. Piemenov, Fusion Sci. Technol. **51**, 655 (2007).
[95]I. V. Akimova, A. A. Akunets, L. A. Borisenko, A. I. Gromov, Y. A. Merkuliev, and A. S. Orekhov, J. Radioanal. Nucl. Chem. **299**, 955 (2014).
[96]M. Nagata, T. Norimatsu, M. Nakai, K. Nagai, N. Ueda, S. Fujioka, T. Aota, H. Nishimura, K. Nishihara, N. Miyanaga, Y. Izawa, and K. Mima, Jpn. J. Appl. Phys., Part 2 **45**, L884 (2006).
[97]P. Hayden, A. Cummings, N. Murphy, G. O'Sullivan, P. Sheridan, J. White, and P. Dunne, J. Appl. Phys. **99**, 093302 (2006).
[98]D. Faith, W. Nazarov, and C. Horsfield, Fusion Sci. Technol. **45**, 90 (2004).
[99]W. Nazarov and P. G. McGivern, Fusion Technol. **38**, 110 (2000).
[100]N. Miele-Pajot, L. G. Hubert-Pfalzgraf, R. Papiernik, J. Vaissermann, and R. Collier, J. Mater. Chem. **9**, 3027 (1999).
[101]F. Ito, N. Nakamura, T. Norimatsu, and K. Nagai, Plasma Fusion Res. **4**, S1011 (2009).
[102]T. Fujimura, T. Norimatsu, M. Nakai, K. Nagai, A. Iwamoto, and K. Mima, Fusion Sci. Technol. **51**, 677 (2007).
[103]R. B. Randolph, J. A. Oertal, D. W. Schmidt, M. N. Lee, K. H. Henderson, and C. E. Hamilton, Fusion Sci. Technol. **70**, 230 (2016).
[104]K. A. DeFriend, R. D. Day, D. Hatch, B. F. Espinoza, S. Feng, and B. M. Patterson, Fusion Sci. Technol. **55**, 490 (2009).
[105]J. Andre, R. Botrel, J. Schunck, A. Pinay, C. Chicanne, and M. Theobald, Fusion Sci. Technol. **70**, 237 (2016).
[106]T. Norimatsu, K. Nagai, T. Takeda, and K. Mima, Fusion Sci. Technol. **43**, 339 (2003).
[107]H. Homma, H. Kadota, H. Hosokawa, M. Nagata, T. Fujimura, K. Nagai, M. Nakai, T. Norimatsu, and H. Azechi, Fusion Sci. Technol. **59**, 276–278 (2011).
[108]K. A. DeFriend, B. F. Espinoza, A. Nobile, K. V. Salazar, R. D. Day, N. E. Elliott, T. H. Pierce, J. E. Elliott, D. W. Schmidt, F. Fierro, D. Sandoval, J. F. Griego, A. C. Valdez, and M. Droege, Fusion Sci. Technol. **49**, 701 (2006).
[109]K. A. DeFriend, B. Espinoza, and B. Patterson, Fusion Sci. Technol. **51**, 693 (2007).
[110]R. R. Paguio, J. F. Hund, B. E. Blue, D. G. Schroen, K. M. Saito, C. A. Frederick, R. J. Strauser, and K. Quan, Fusion Sci. Technol. **55**, 450 (2009).
[111]W. Nazarov, Fusion Sci. Technol. **41**, 193 (2002).
[112]N. G. Borisenko, A. I. Gromov, Y. A. Merku'ev, A. V. Mitrifanov, and W. Nazarov, Fusion Technol. **38**, 115 (2000).
[113]Q. Liu, F. Ye, Z. Hou, S. Liu, Y. Geo, and H. Zhang, J. Eur. Ceram. Soc. **33**, 2421 (2013).
[114]F. Ito, K. Nagai, M. Nakai, T. Norimatsu, A. Nikitenko, S. Tolokonnikov, E. Koresheva, T. Fujimura, H. Azachi, and K. Mima, Jpn. J. Appl. Phys., Part 2 **45**, L335 (2006).
[115]F. Ito, K. Nagai, M. Nakai, and T. Norimatsu, Fusion Sci. Technol. **49**, 663 (2006).
[116]S. M. Lambert, G. E. Overturf, G. Wilemski, S. A. Letts, D. Schroen-Carey, and R. C. Cook, J. Appl. Polym. Sci. **65**, 2111 (1997).
[117]F. Ito, K. Nagai, M. Nakai, and T. Norimatsu, Macromol. Chem. Phys. **206**, 2171 (2005).
[118]M. Bono, D. Bennett, C. Castro, J. Satcher, J. Poco, B. Brown, H. Martz, N. Teslich, R. Hibbard, A. Hamza, P. Amendt, H. Robey, J. Milovich, and R. Walance, Fusion Sci. Technol. **51**, 611 (2007).
[119]S. W. Haan, P. A. Amendt, D. A. Callhan, T. R. Dittrich, M. J. Edwards, B. A. Hammel, D. D. Ho, D. S. Jones, J. D. Lindl, M. M. Marinak, D. H. Munro, S. M. Pollaine, J. D. Salmonson, B. K. Spears, and L. J. Suter, Fusion Sci. Technol. **51**, 509 (2007).
[120]R. R. Paguio, M. Takagi, M. Thi, J. F. Hund, A. Nikroo, S. Paguio, R. Luo, A. L. Greenwood, O. Acenas, and S. Chowdhury, Fusion Sci. Technol. **51**, 682 (2007).
[121]C. Lattaud, L. Guillot, C.-H. Brachais, E. Fleury, O. Legaie, and J.-P. Couvercelle, J. Appl. Polym. Sci. **124**, 4882 (2012).
[122]R. R. Paguio, D. Jaison, K. M. Saito, K. Quan, J. F. Hund, and A. Nikroo, Fusion Sci. Technol. **59**, 199 (2011).
[123]H. Yang, K. Nagai, M. Nakai, and T. Norimatsu, Laser Part. Beams **26**, 449 (2008).
[124]K. Nagai, H. Yang, T. Norimatsu, H. Azechi, F. Belkada, Y. Fujimoto, T. Fujimura, K. Fujioka, S. Fujioka, H. Homma, F. Ito, A. Iwamoto, T. Jitsuno, Y. Kaneyasu, M. Nakai, N. Nemoto, H. Saika, T. Shimoyama, Y. Suzuki, K. Yamanaka, and K. Mima, Nucl. Fusion **49**, 095028 (2009).
[125]K. Nagai, H. Azechi, F. Ito, A. Iwamoto, Y. Izawa, T. Johzaki, R. Kodama, K. Mima, T. Mito, M. Nakai, N. Nemoto, T. Norimatsu, Y. Ono, K. Shigemori, H. Shiraga, and K. A. Tanaka, Nucl. Fusion **45**, 1277 (2005).
[126]See http://www.inovenso.com for information about electrospinning device.
[127]C. Pan, Z.-Z. Gu, K. Nagai, Y. Shimada, K. Hashimoto, T. Birou, and T. Norimatsu, J. Appl. Phys. **100**, 016104 (2006).
[128]K. Nagai, K. Miyamato, T. Iyoda, C. Pan, and Z. Gu, Fusion Sci. Technol. **59**, 216 (2011).
[129]L. J. Jiang, J. H. Campbell, Y. F. Lu, T. Bernat, and N. Petta, Fusion Sci. Technol. **70**, 295 (2016).
[130]J. S. Oakdale, R. F. Smith, J.-B. Forien, W. L. Smith, S. J. Ali, L. B. B. Aji, T. M. Willey, J. Ye, A. W. van Buuren, M. A. Worthington, S. T. Prisbrey, H.-S. Park, P. A. Arnendt, T. F. Baumann, and J. Biener, Adv. Funct. Mater. **27**, 1702425 (2017).
[131]A. Nikroo, D. Czechowics, R. Paguio, A. L. Greenwood, and M. Takagi, Fusion Sci. Technol. **45**, 84 (2004).
[132]F. Ito, N. Nakamura, K. Nagai, M. Nakai, and T. Norimatsu, Fusion Sci. Technol. **55**, 465 (2009).
[133]J. J. Karnes, N. M. Petta, and J. E. Streit, Fusion Sci. Technol. **55**, 472 (2009).
[134]Q. Gu, K. Nagai, T. Norimatsu, S. Fujioka, H. Nishimura, K. Nishihara, N. Miyanaga, and Y. Izawa, Chem. Mater. **17**, 1115 (2005).
[135]K. Nagai, Q.-C. Gu, Z.-Z. Gu, T. Okuno, S. Fujioka, H. Nishimura, Y.-Z. Tao, Y. Yasuda, M. Nakai, T. Norimatsu, Y. Shimada, M. Yamaura, H. Yoshida, M. Nakatsuka, N. Miyanaga, K. Nishihara, and Y. Izawa, Appl. Phys. Lett. **88**, 094102 (2006).
[136]M. J. Bono, G. Q. Langstaff, O. Cervantes, C. M. Akaba, S. R. Strodtbeck, A. V. Hamza, N. E. Teslich, R. J. Foreman, J. P. Lotscher, G. W. Nyce, R. H. Page, T. R. Dittrich, and G. Glendinning, Fusion Sci. Technol. **55**, 319 (2009).
[137]K. Nagai, D. Wada, M. Nakai, and T. Norimatsu, Fusion Sci. Technol. **49**, 686 (2006).
[138]K. Nagai, Q.-C. Gu, T. Norimatsu, S. Fujioka, H. Nishimura, N. Miyanaga, K. Nishihara, Y. Izawa, and K. Mima, Laser Part. Beams **26**, 497 (2008).
[139]C. Sun, X.-W. Zhao, Y.-J. Zhao, R. Zhu, and Z.-Z. Gu, Plasma Fusion Res. **4**, S1009 (2009).
[140]H. Masuda and K. Fukuda, Science **268**, 1466 (1995).
[141]W. Lee and S.-J. Park, Chem. Rev. **114**, 7487 (2014).
[142]N. Yamashita, H. Komiyama, Y. Zhao, M. Komura, T. Iyoda, and K. Nagai, Jpn. J. Appl. Phys., Part 1 **51**, 076704 (2012).
[143]T. Yang, S. Zhang, M. Komura, T. Iyoda, and K. Nagai, Jpn. J. Appl. Phys., Part 1 **51**, 070201 (2012).
[144]M. Komura, K. Kamata, T. Iyoda, and K. Nagai, Fusion Sci. Technol. **63**, 257 (2013).
[145]M. Komura, H. Komiyama, K. Nagai, and T. Iyoda, Macromolecules **46**, 9013 (2013).
[146]N. Yamashita, S. Watanabe, K. Nagai, M. Komura, T. Iyoda, K. Aida, Y. Tada, and H. Yoshida, J. Mater. Chem. C **3**, 2837 (2015).
[147]M. A. Hoque, H. Komiyama, H. Nishiyama, K. Nagai, T. Kawauchi, and T. Iyoda, J. Polym. Sci., Part A: Polym. Chem. **54**, 1175 (2016).
[148]K. Kamata, Z. Piao, S. Suzuki, T. Fujimori, W. Tajiri, K. Nagai, T. Iyoda, A. Yamada, T. Hayakawa, M. Ishiwara, S. Haraguchi, A. Belay, T. Tanaka, K. Takana, K. Takano, and M. Hangyo, Sci. Rep. **4**, 4919 (2014).
[149]M. Dalui, M. Kundu, T. M. Trivikram, R. Rajeev, K. Ray, and M. Krishnamurthy, Sci. Rep. **4**, 6002 (2014).

[150]C. E. Hamilton, D. Honnell, B. M. Patterson, D. W. Schmidt, and K. A. D. Obrey, Fusion Sci. Technol. **59**, 194 (2011).
[151]L. J. Peacock, C. D. Bentley, N. Basin, E. Stott, and C. MacQueen, Fusion Sci. Technol. **59**, 190 (2011).
[152]K. K. Dannenberg, C. A. Back, C. A. Frederick, E. M. Giraldez, R. R. Holt, W. J. Krych, D. G. Schroen, and C. O. Russell, Fusion Sci. Technol. **51**, 673 (2007).
[153]C. W. Barnes, R. D. Day, N. E. Elliott, B. H. Batha, N. E. Lainer, G. R. Margelssen, J. M. Scott, S. Rothman, C. Horsfield, A. M. Dunne, and K. W. Porter, Fusion Sci. Technol. **41**, 203 (2002).
[154]D. Faith, C. J. Horsfield, and W. Nazarov, J. Mater. Sci. **41**, 3973 (2006).
[155]R. W. Pekala and D. W. Schaefer, Macromolecules **26**, 5487 (1993).
[156]L. H. Sperling, *Introduction to Physical Polymer Science*, 4th ed. (Wiley, 2006).